

New A-site Ordered Perovskite Cobaltite $\text{LaBaCo}_2\text{O}_6$: Synthesis, Structure, Physical Property and Cation Order–Disorder Effect

Tomohiko NAKAJIMA*, Masaki ICHIHARA and Yutaka UEDA

*Materials Design and Characterization Laboratory, Institute for Solid State Physics,
The University of Tokyo, 5-1-5 Kashiwanoha, Kashiwa, Chiba 277-8581*

(Received January 13, 2005; accepted March 9, 2005)

By means of annealing $\text{LaBaCo}_2\text{O}_5$ under high pressure oxygen, we have successfully synthesized a new A-site ordered perovskite cobaltite, $\text{LaBaCo}_2\text{O}_6$. The structure and electromagnetic properties of $\text{LaBaCo}_2\text{O}_6$ have been investigated and compared to those of the ordinary A-site disordered $\text{La}_{0.5}\text{Ba}_{0.5}\text{CoO}_3$. Both $\text{LaBaCo}_2\text{O}_6$ and $\text{La}_{0.5}\text{Ba}_{0.5}\text{CoO}_3$ have mixed states of low-spin and intermediate-spin states and show metallic behaviors generated by double exchange interaction. $\text{LaBaCo}_2\text{O}_6$ has a ferromagnetic transition at $T_C = 175$ K, which is lower by 15 K than T_C of $\text{La}_{0.5}\text{Ba}_{0.5}\text{CoO}_3$. At around 140 K, some structural changes are observed in both compounds and below the temperature they exhibit magnetic glassy (cluster glass) behaviors, accompanied by the gradual change to insulating or semiconductive behaviors. The refined structural data and magnetic and electrical properties suggest a partial $d_{x^2-y^2}$ orbital ordering for $\text{LaBaCo}_2\text{O}_6$ below 140 K, in contrast to a partial $d_{3z^2-r^2}$ orbital ordering for $\text{La}_{0.5}\text{Ba}_{0.5}\text{CoO}_3$.

KEYWORDS: A-site ordered/disordered perovskite cobaltites, Low spin and intermediate spin states, ferromagnetic metal, structural change, partial orbital ordering

DOI: 10.1143/JPSJ.74.1572

1. Introduction

In the last decade, perovskite cobaltites with the general formula $(R_{1-x}A_x^{3+}A_x^{2+})\text{CoO}_3$ (R = rare earth elements and A = alkaline earth elements) have received much attention because of their enchanting physical properties such as metal–insulator (MI) transition and spin configuration change.^{1–6)} The spin configuration change is one of the remarkable phenomena characteristic of cobalt oxides. LaCoO_3 which is a good illustration^{2,3)} has nonmagnetic Co^{3+} ($3d^6$) ions with the low-spin (LS) state configuration ($t_{2g}^6, S = 0$) below 100 K, and then the LS state gradually change to the intermediate-spin (IS) state ($t_{2g}^5e_g^1, S = 1$) with increase of temperature. Finally, it changes to the high-spin (HS) state ($t_{2g}^4e_g^2, S = 2$) above 550 K. This is caused by the competition between the crystal field splitting Δ_C and the exchange energy Δ_E for $3d$ electrons and the occupied orbitals in CoO_6 octahedron. The Δ_C and Δ_E are controlled by choosing the combination of A-site cations, R^{3+} and A^{2+} with various ionic radii.⁴⁾

It is well known that the A-site cation modification in the perovskite oxides plays a very important role for the control of their physical properties. Very recently, we have verified the A-site randomness effect on perovskite manganites from the comparison of structural and physical properties between the A-site disordered $R_{0.5}\text{Ba}_{0.5}\text{MnO}_3$ and ordered RBaMn_2O_6 .^{7,8)} It has been revealed that not only A-site randomness but also structural two-dimensionality produced by the layer ordering of A-site cations significantly influence physical properties of perovskite manganites; the exclusion of structural randomness particularly enhances charge-orbital order and magnetic long-range ordering, and moreover the

structural two-dimensionality stabilizes the layer type $d_{x^2-y^2}$ orbital ordering in $\text{PrBaMn}_2\text{O}_6$ and $\text{NdBaMn}_2\text{O}_6$.⁸⁾ This indicates that the order-disorder of A-site cations is one of reliable factors to control physical properties. Fortunately, perovskite cobaltites also have the A-site layer-type ordered compound, $\text{RBaCo}_2\text{O}_{5+x}$.^{9–12)} These A-site ordered cobalt oxides are oxygen deficient perovskite compounds with a wide range of oxygen non-stoichiometry and various oxygen-vacancy ordering. In order to make randomness effect clear, it is crucial to obtain the stoichiometric compound, RBaCo_2O_6 . However there has been no report of the fully oxidized A-site ordered cobaltites.

In this work, we have successfully synthesized a new A-site layer-type ordered $\text{LaBaCo}_2\text{O}_6$ and the ordinary disordered $\text{La}_{0.5}\text{Ba}_{0.5}\text{CoO}_3$. In the present paper, the structures and electromagnetic properties of $\text{LaBaCo}_2\text{O}_6$ are reported and compared to those of $\text{La}_{0.5}\text{Ba}_{0.5}\text{CoO}_3$. We also discuss how the A-site order–disorder affects the structural and physical properties of perovskite cobaltites.

2. Experimental

Polycrystalline sample of the A-site ordered $\text{LaBaCo}_2\text{O}_6$ was prepared by a similar synthesis procedure of the A-site ordered manganites.^{7,8)} Mixed powder of starting materials, La_2O_3 , BaCO_3 and CoO , in an appropriate molar ratio was ground, pressed into a pellet and heated at 1173–1423 K in Ar gas for 48 h, which yielded the A-site ordered and oxygen-deficient $\text{LaBaCo}_2\text{O}_{6-x}$ ($x \sim 1.0$). For the full oxidation, $x = 0.0$, the obtained sample was annealed at low temperature of 623 K in high-pressure O_2 gas ($P \sim 200$ atm) for 6 h. Thermogravimetric analysis by the reduction in H_2 confirmed the stoichiometric oxygen content of $\text{LaBaCo}_2\text{O}_{6.00}$. A slight oxygen-deficiency remained without the high-pressure oxygen annealing, and the annealing of $\text{LaBaCo}_2\text{O}_6$ under O_2 gas at high temperatures resulted in the disorder of La/Ba cations. Except $\text{LaBaCo}_2\text{O}_6$, we could not obtain the fully oxidized A-site ordered cobaltites

*Present address: Materials Design and Characterization Laboratory, Institute for Solid State Physics, The University of Tokyo, 5-1-5 Kashiwanoha, Kashiwa, Chiba 277-8581.
E-mail: t-nakaji@issp.u-tokyo.ac.jp

$RBaCo_2O_6$ (R = rare earth elements) in the same condition of 200 atm oxygen pressure. The A-site disordered $La_{0.5}Ba_{0.5}CoO_3$ was synthesized by literature methods.^{4,13} The crystal structures were refined by the Rietveld analysis of powder neutron diffraction using RIETAN2000.¹⁴ The neutron powder diffraction experiments were conducted for $T = 20\text{--}300$ K using the Kinken powder diffractometer for high efficiency and high resolution measurements, HERMES, at Institute for Materials Research (IMR), Tohoku University, installed at the JRR-3M reactor in Japan Atomic Energy Research Institute (JAERI), Tokai, Japan. Neutrons with a wavelength of 1.8207 \AA were obtained by the 331 reflection of the Ge monochromator. The $12'$ -blank-sample- $18'$ collimation was employed. The magnetic properties were studied using a SQUID magnetometer in a temperature range $T = 2\text{--}400$ K. The electric resistivity of a sintered pellet was measured for $T = 2\text{--}400$ K by a conventional four-probe technique.

3. Results and Discussion

Figure 1 shows neutron powder diffraction patterns of (a) $LaBaCo_2O_6$ and (b) $La_{0.5}Ba_{0.5}CoO_3$ at 300 K. In $LaBaCo_2O_6$, the 001 reflection around $2\theta = 13^\circ$ indicates a layer-type ordering of La/Ba cations (the inset of Fig. 1), and all of the observed diffraction peaks can be indexed in the space group $P4/mmm$ with the lattice parameters

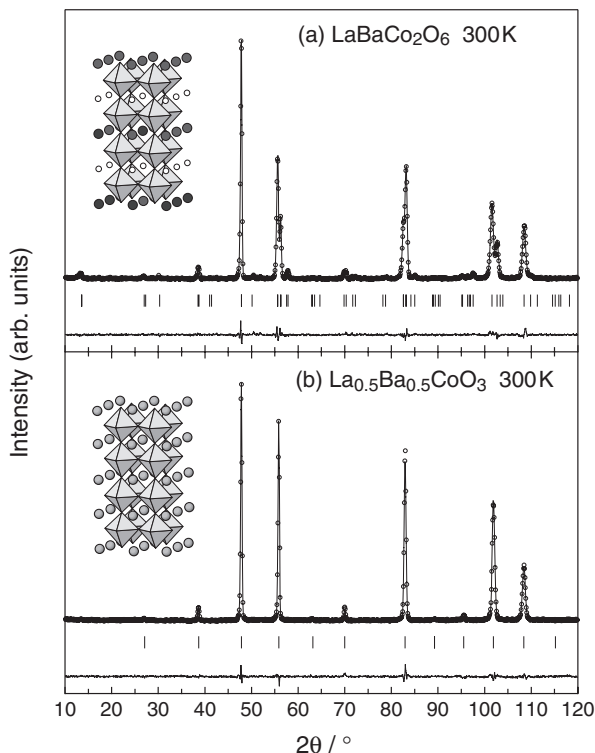


Fig. 1. The neutron diffraction patterns of (a) $LaBaCo_2O_6$ and (b) $La_{0.5}Ba_{0.5}CoO_3$ at 300 K. The calculated and observed diffraction profiles are shown at the top with the solid line and the cross markers, respectively. The vertical marks in the middle show positions calculated for Bragg reflections. The lower trace is a plot of the difference between calculated and observed intensities. Data are refined in space group (a) $P4/mmm$ and (b) $Pm\bar{3}m$. The schematic crystal structure is illustrated in each figure by using the corner-shared CoO_6 octahedra and A-site cations, where the open and solid balls in (a) are La and Ba ions, respectively, and the shadowed balls in (b) are the mixture of them.

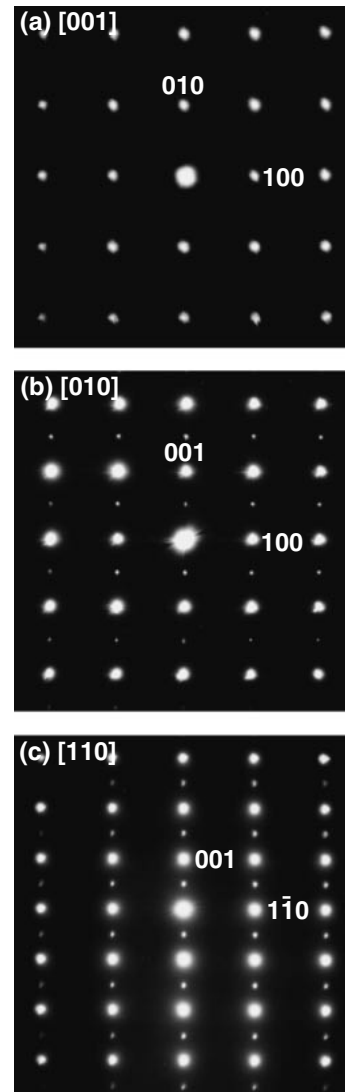


Fig. 2. The electron diffraction patterns of $LaBaCo_2O_6$ at room temperature taken along the zone axes: (a) [001], (b) [010] and (c) [110].

$a = 3.89984(7) \text{ \AA}$, $c = 7.7145(2) \text{ \AA}$, $V = 117.329(4) \text{ \AA}^3$. The electron diffraction of $LaBaCo_2O_6$ shown in Fig. 2 also clearly shows the doubling of the c -axis and a tetragonal symmetry with $a_p \times a_p \times 2c_p$ unit cell, where a_p and c_p represent lattice parameters for the simple perovskite structure. Table I(a) shows the refined structural data of $LaBaCo_2O_6$ at 300 K. The a is much longer than the $c/2$. Moreover, the CoO_6 octahedra have asymmetric (noncentrosymmetric) distortion [see the inset of Fig. 3(a)] as seen in the A-site ordered manganites.^{8,15,16} Namely the CoO_2 square plane is extended by chemical pressure of the larger BaO layer and shifted to the smaller LaO layer; two apical Co–O1 and Co–O3 distances are $1.916(8) \text{ \AA}$ and $1.941(8) \text{ \AA}$, respectively, and planar four Co–O2 distances are $1.9524(4) \text{ \AA}$. Thus, $LaBaCo_2O_6$ have apically compressed CoO_6 octahedra at room temperature, although the shape is asymmetric along the c -axis. Figure 3(a) shows lattice parameters, bond distances and bond angle of $LaBaCo_2O_6$ as a function of temperature. On cooling, both a and $c/2$ monotonically shrink down to 140 K and below the temperature the degree of the shrinkage become less. Between the two apical Co–O distances, the longer Co–O3 distance

Table I. Refined structural parameters and selected bond distances and angles of (a) LaBaCo₂O₆ and (b) La_{0.5}Ba_{0.5}CoO₃.

(a) LaBaCo ₂ O ₆			
Space group: $P4/mmm$	La	1a	$B_{\text{iso}} = 0.50(8) \text{ \AA}^2$
$a = 3.89984(7) \text{ \AA}$	Ba	1b	$B_{\text{iso}} = 0.50(8) \text{ \AA}^2$
$c = 7.7145(2) \text{ \AA}$	Co	2h	$z = 0.248(1)$
$V = 117.329(4) \text{ \AA}^3$			$B_{\text{iso}} = 0.14(5) \text{ \AA}^2$
$R_{\text{wp}} = 7.58\%$	O1	1c	$B_{\text{iso}} = 1.14(9) \text{ \AA}^2$
$R_{\text{e}} = 6.03\%$	O2	4i	$z = 0.2356(3)$
$R_{\text{I}} = 1.46\%$			$B_{\text{iso}} = 0.84(6) \text{ \AA}^2$
$R_{\text{F}} = 2.76\%$	O3	1d	$B_{\text{iso}} = 0.70(9) \text{ \AA}^2$
Distances		Angles	
Co–O1 = 1.916(8) \AA		Co–O1–Co = 180°	
Co–O2 = 1.9524(4) \AA		Co–O2–Co = 174.2(5)°	
Co–O3 = 1.941(8) \AA		Co–O3–Co = 180°	
(b) La _{0.5} Ba _{0.5} CoO ₃			
Space group: $Pm\bar{3}m$	La/Ba	1a	$B_{\text{iso}} = 0.67(8) \text{ \AA}^2$
$a = 3.88813(4) \text{ \AA}$	Co	1b	$B_{\text{iso}} = 0.46(8) \text{ \AA}^2$
$V = 58.779(1) \text{ \AA}^3$	O	3c	$B_{\text{iso}} = 1.30(9) \text{ \AA}^2$
$R_{\text{wp}} = 7.76\%$			
$R_{\text{e}} = 6.25\%$			
$R_{\text{I}} = 3.42\%$			
$R_{\text{F}} = 3.52\%$			
Distance		Angle	
Co–O = 1.9441 \AA		Co–O–Co = 180°	

decreases with decreasing temperature, while the shorter Co–O1 distance scarcely changes as well as the Co–O2 distances. As a result, the Co–O3 distance is close to the Co–O1 distance around 140 K and below the temperature both distances become temperature-independent. This means that the noncentrosymmetric distortion of apically compressed CoO₆ octahedron changes to a centrosymmetric one below 140 K.

The neutron diffraction pattern of La_{0.5}Ba_{0.5}CoO₃ can be indexed in a primitive cubic perovskite cell with the space group $Pm\bar{3}m$. There is no extra peak suggesting any superstructures. It should be noted that the diffraction peak around $2\theta = 13^\circ$ observed in LaBaCo₂O₆ is absent in La_{0.5}Ba_{0.5}CoO₃. The lattice parameter of La_{0.5}Ba_{0.5}CoO₃ is determined to be $a = 3.88813(4) \text{ \AA}$ and $V = 58.779(1) \text{ \AA}^3$. Concerning the low temperature structure of La_{0.5}Ba_{0.5}CoO₃, Fauth *et al.* reported the transition to a tetragonal phase below 180 K, accompanied by a Jahn–Teller (JT) distortion of CoO₆ octahedra.¹³ Figure 3(b) shows the temperature dependence of lattice parameters for La_{0.5}Ba_{0.5}CoO₃. The crystal structure of La_{0.5}Ba_{0.5}CoO₃ slightly changes from cubic ($Pm\bar{3}m$) to tetragonal ($P4/mmm$) below about 140 K, agreeing with the previous work.¹³ Below 140 K, the a is shorter than the c , which originates from the elongation of CoO₆ octahedra along the apical oxygen direction, as shown in Fig. 3(b).

Figure 4 shows the magnetic susceptibilities (M/H) measured under 0.1 T for (a) LaBaCo₂O₆ and (b) La_{0.5}Ba_{0.5}CoO₃. LaBaCo₂O₆ shows a paramagnetic behavior, obeying a Curie–Weiss law with effective moment $P_{\text{eff}} = 2.81(2) \mu_{\text{B}}$ and Weiss constant $\theta_0 = 208.0(7) \text{ K}$ between 280 K and

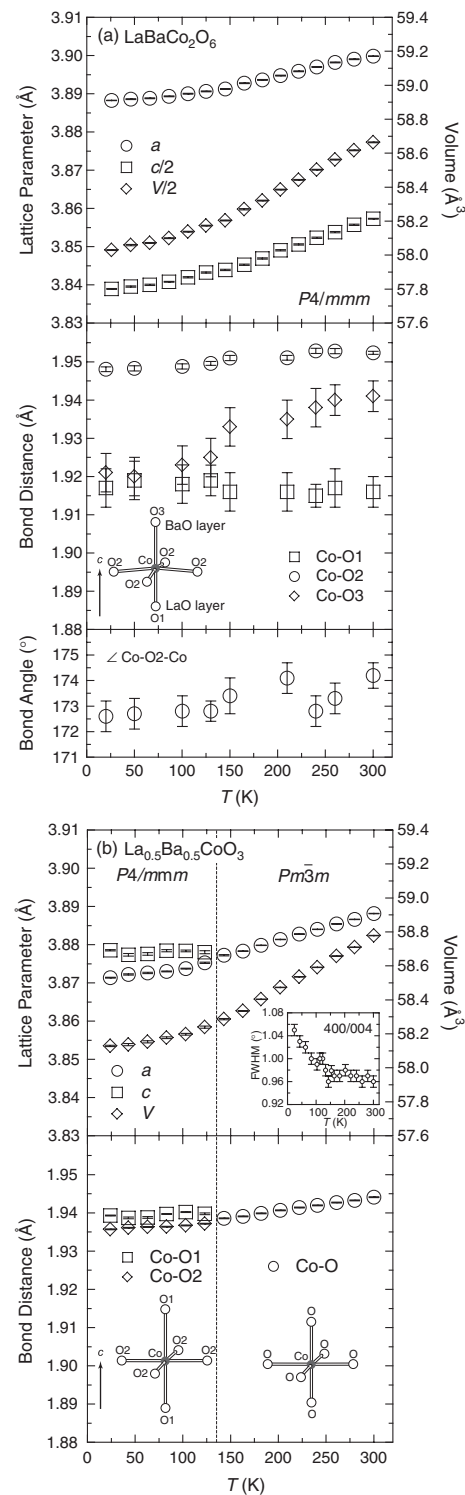


Fig. 3. The temperature dependence of lattice parameters, bond distances and bond angle for (a) LaBaCo₂O₆ and (b) La_{0.5}Ba_{0.5}CoO₃. The inset in (b) shows the peak width of selected reflection from powder neutron diffraction data, as a function of temperature.

400 K. The value of $P_{\text{eff}} = 2.81(2) \mu_{\text{B}}$ indicates a mixed spin state of IS and LS states for Co^{3.5+} (Co³⁺/Co⁴⁺). A ferromagnetic interaction represented as a positive Weiss constant $\theta_0 = 208.0(7) \text{ K}$ could be due to the double exchange (DE) interaction generated by e_g -electrons in IS state. Actually at $T_{\text{C}} = 175 \text{ K}$, LaBaCo₂O₆ exhibits a ferromagnetic transition, accompanying with a sharp increase of M/H but without any structural change. Succes-

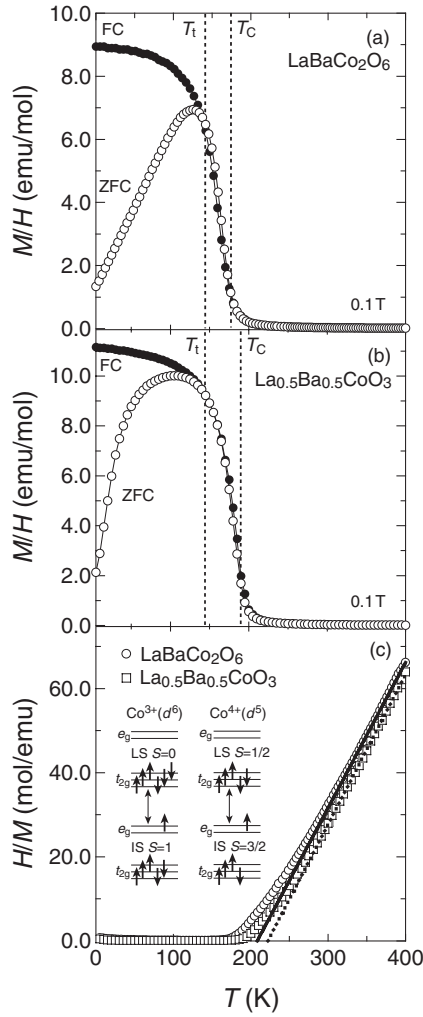


Fig. 4. The temperature dependence of magnetic susceptibilities for (a) $\text{LaBaCo}_2\text{O}_6$ and (b) $\text{La}_{0.5}\text{Ba}_{0.5}\text{CoO}_3$ under 0.1 T on zero-field cooled (ZFC) and field cooled (FC) processes. The inverse magnetic susceptibility vs temperature plots are shown in (c) with the spin configurations of low spin (LS) and intermediate spin (IS) states for Co^{3+} and Co^{4+} , where the solid and dotted lines represent the Curie-Weiss fittings for $\text{LaBaCo}_2\text{O}_6$ and $\text{La}_{0.5}\text{Ba}_{0.5}\text{CoO}_3$, respectively.

sively it shows a magnetic transition around 140 K below which a significant difference of $M/H-T$ curves is observed between zero field cooled (ZFC) and field cooled (FC) processes. A similar cluster glass behavior was reported in $\text{La}_{1-x}\text{Sr}_x\text{CoO}_3$ ($0.18 \leq x \leq 0.50$) by Itoh *et al.*^{17,18} Such cluster glass behavior could occur as a result of the competition between randomly distributed ferromagnetic and antiferromagnetic interactions. This magnetic transition corresponds to the structural change around 140 K. On the other hand, $\text{La}_{0.5}\text{Ba}_{0.5}\text{CoO}_3$ also shows similar behaviors; a paramagnetic behavior with $P_{\text{eff}} = 2.95(1) \mu_B$ and Weiss constant $\theta_{\text{do}} = 221.6(5) \text{ K}$, a ferromagnetic transition at $T_C = 190 \text{ K}$ and a cluster glass transition around 140 K. Below 140 K, the neutron diffraction study reveals that both compounds show only ferromagnetic peaks and no antiferromagnetic ones. It is worth to note that T_C of $\text{LaBaCo}_2\text{O}_6$ is 15 K lower than that of $\text{La}_{0.5}\text{Ba}_{0.5}\text{CoO}_3$. This is different from the case of perovskite manganites in which the suppression of structural disorder is great advantage to the hopping of e_g -electrons generated by DE interaction,^{8,19}

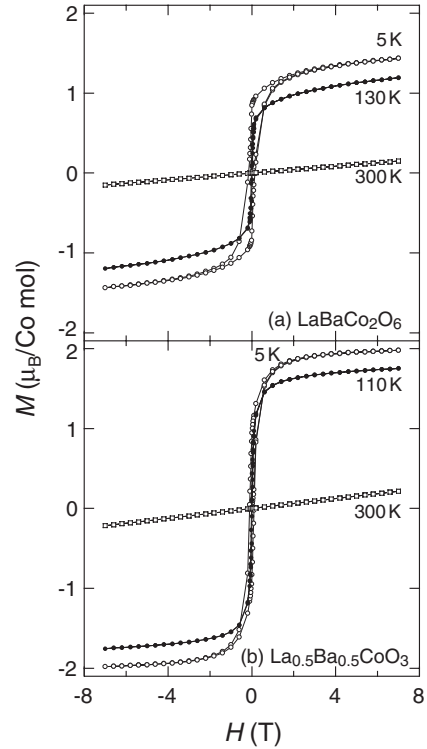


Fig. 5. The magnetization curves of (a) $\text{LaBaCo}_2\text{O}_6$ and (b) $\text{La}_{0.5}\text{Ba}_{0.5}\text{CoO}_3$ at 5, 130 and 300 K.

resulting in the increase of T_C . Figure 5 shows the magnetization curves of (a) $\text{LaBaCo}_2\text{O}_6$ and (b) $\text{La}_{0.5}\text{Ba}_{0.5}\text{CoO}_3$ at 5, 130 and 300 K. At 5 K, the saturation moments of $\text{LaBaCo}_2\text{O}_6$ and $\text{La}_{0.5}\text{Ba}_{0.5}\text{CoO}_3$ are $1.5 \mu_B/\text{Co}$ and $2.0 \mu_B/\text{Co}$, respectively. This means that the spin states of both compounds are mixed states of LS and IS states also in the magnetically ordered states and however LS state is more dominant in $\text{LaBaCo}_2\text{O}_6$ than in $\text{La}_{0.5}\text{Ba}_{0.5}\text{CoO}_3$.

Figure 6 shows the temperature variations of electrical resistivity measured at 0 and 9 T and magnetoresistance (MR) effect at 9 T for (a) $\text{LaBaCo}_2\text{O}_6$ and (b) $\text{La}_{0.5}\text{Ba}_{0.5}\text{CoO}_3$. The MR (%) is given by $\text{MR} (\%) = \{[\rho(0) - \rho(H)] / \rho(H)\} \times 100\%$ where $\rho(H)$ is electrical resistivity at 9 T and $\rho(0)$ at zero magnetic field. The resistivity (ρ_0) of $\text{LaBaCo}_2\text{O}_6$ exhibits a metallic behavior between 125 and 400 K, and it gradually changes to semiconductive one below 125 K. The magnetic field dependence of resistivity is not observed at low temperature but slightly observed around T_C , as shown in Fig. 6(a). The resistivity (ρ_{do}) of $\text{La}_{0.5}\text{Ba}_{0.5}\text{CoO}_3$ also shows a metallic behavior down to 140 K, and then it increases with decreasing temperature below 140 K. The ρ_{do} runs up to a tenfold value of ρ_0 at 2 K and moreover a large MR effect is observed below 100 K.

The metallic behaviors of both $\text{LaBaCo}_2\text{O}_6$ and $\text{La}_{0.5}\text{Ba}_{0.5}\text{CoO}_3$ can be described as the hopping of e_g -electrons generated by DE interaction, which is evident from positive Weiss constants in the paramagnetic states and ferromagnetic transitions. The values of P_{eff} in the paramagnetic states and magnetization in the magnetically ordered states indicate mixed spin states of LS and IS on $\text{Co}^{3.5+}$ ($\text{Co}^{3+}/\text{Co}^{4+}$) in both $\text{LaBaCo}_2\text{O}_6$ and $\text{La}_{0.5}\text{Ba}_{0.5}\text{CoO}_3$, where the expected electron configurations are LS (t_{2g}^6 , $S = 0$) and IS ($t_{2g}^5 e_g^1$, $S = 1$) for Co^{3+} and LS (t_{2g}^5 , $S = 1/2$) and IS ($t_{2g}^4 e_g^1$,

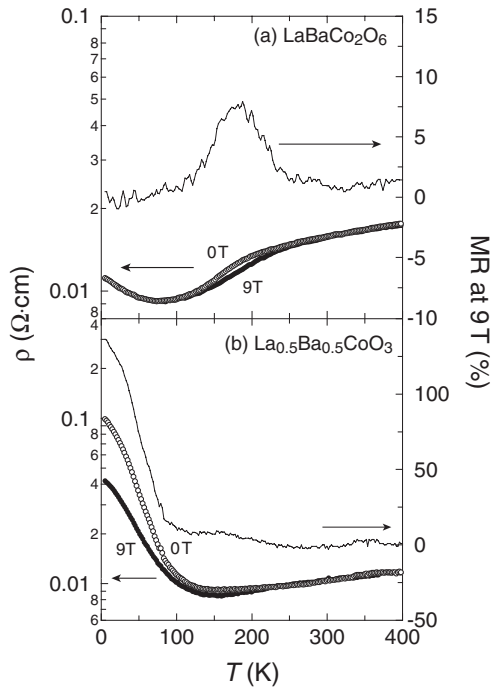


Fig. 6. The temperature dependence of electrical resistivity at 0 and 9 T and magnetoresistance (MR) for (a) LaBaCo₂O₆ and (b) La_{0.5}Ba_{0.5}CoO₃.

$S = 3/2$) for Co⁴⁺. We have not exactly determined the electron configurations of each ion. However, it is thought that the IS and LS states are dominant in Co³⁺ and Co⁴⁺ ions respectively, because the DE interaction functions in such states much more effectively. This is consistent with the magnitude of saturation moment. The smaller P_{eff} and saturation moment in LaBaCo₂O₆ tell us a little larger ratio of LS state or a smaller amount of e_g -electron in it. LaBaCo₂O₆ has a smaller unit cell volume than La_{0.5}Ba_{0.5}CoO₃, and the increasing Δ_C increases LS population and decreases e_g -electrons. This might be a cause of the lowering of T_C by 15 K in LaBaCo₂O₆, in contrast to the case of LaBaMn₂O₆ ($T_C = 330$ K) and La_{0.5}Ba_{0.5}MnO₃ ($T_C = 280$ K). The number of e_g -electron is equal in LaBaMn₂O₆ and La_{0.5}Ba_{0.5}MnO₃, therefore, the absence of structural disorder in LaBaMn₂O₆ enhances ferromagnetic transition.

Such mixed spin states of LS and IS could be related to magnetic glassy states at low temperatures. Both LaBaCo₂O₆ and La_{0.5}Ba_{0.5}CoO₃ transform to magnetic glassy states below about 140 K. The magnetic transitions are accompanied by the structural changes. Fauth *et al.* proposed that the structural distortion from cubic to tetragonal in La_{0.5}Ba_{0.5}CoO₃ is due to the partial $d_{3z^2-r^2}$ -type orbital ordering.¹³ This is supported by the present results of structural refinement, namely the elongation of CoO₆ octahedra along the apical oxygen direction is consistent to the $d_{3z^2-r^2}$ -type orbital ordering. The $d_{3z^2-r^2}$ -type orbital ordering results in the change of magnetic interaction into an antiferromagnetic one from the ferromagnetic one generated by DE interaction. The e_g -electrons in IS state of Co^{3.5+} (Co³⁺/Co⁴⁺) is responsible for the $d_{3z^2-r^2}$ -type orbital ordering. In a mixed state of LS and IS, the $d_{3z^2-r^2}$ -type orbital ordering partially occurs and consequently the competition between randomly distributed ferromagnetic and antiferromagnetic interactions leads to

magnetic glassy state. The sharp increase of resistivity at low temperature is also consistent with the partial $d_{3z^2-r^2}$ orbital ordering, namely the reduced electron hopping path from three- to one-dimension by such orbital ordering results in increase of the resistivity.

A similar scenario can be considered for LaBaCo₂O₆. However the manners of structural change and resistivity at low temperature in LaBaCo₂O₆ are somewhat different from those in La_{0.5}Ba_{0.5}CoO₃; the noncentrosymmetric distortion of apically compressed CoO₆ octahedra becomes close to a centrosymmetric one below 140 K and the increase of resistivity at low temperature is a little. The A-site ordered LaBaCo₂O₆ has the apically compressed and noncentrosymmetric CoO₆ octahedra, which is caused by the structural characteristic that the CoO₂ layer is sandwiched by the two types of rock-salt layer, LaO and BaO, with different lattice sizes. We know that the similar apically compressed octahedra are favorable for the layer-type $d_{x^2-y^2}$ -type orbital ordering and the peculiar (noncentrosymmetric) distortion of MnO₆ octahedra is relaxed by the $d_{x^2-y^2}$ -type orbital ordering in RBaMn₂O₆.^{8,15,16} For example, a similar structural transition with a higher to lower distortion on cooling has been observed in RBaMn₂O₆ ($R = \text{Tb, Dy, Ho}$ and Y).^{7,15} From these considerations, we propose that LaBaCo₂O₆ exhibits the partial $d_{x^2-y^2}$ orbital ordering below 140 K, contrary to the $d_{3z^2-r^2}$ orbital ordering in La_{0.5}Ba_{0.5}CoO₃. The $d_{x^2-y^2}$ orbital ordering associated with A-type antiferromagnetic metal²⁰ well explains magnetic glassy state and a little increase of resistivity at low temperature in LaBaCo₂O₆; the random distribution of the ferromagnetic and the antiferromagnetic interactions and the reduction of electron hopping paths from three- to two-dimension by the partial $d_{x^2-y^2}$ orbital ordering. The increase of magnetization under high magnetic fields in the cluster glass states of both LaBaCo₂O₆ and La_{0.5}Ba_{0.5}CoO₃ suggests the conversion of the partial orbital ordered states to ferromagnetic metal state by magnetic fields. Much more remarkable MR effect in La_{0.5}Ba_{0.5}CoO₃ might be related to more insulative $d_{3z^2-r^2}$ -type orbital ordering. In order to clarify the partial $d_{x^2-y^2}$ and $d_{3z^2-r^2}$ orbital orderings, however, further experiments should be needed and are now in progress.

4. Summary

To summarize, we have successfully synthesized a new A-site ordered perovskite cobaltite, LaBaCo₂O₆ and investigated its structural and physical properties. The obtained results are compared to those of the ordinary A-site disordered La_{0.5}Ba_{0.5}CoO₃. Both LaBaCo₂O₆ and La_{0.5}Ba_{0.5}CoO₃ show metallic behaviors generated by DE interaction and ferromagnetic transitions at $T_C = 175$ K (LaBaCo₂O₆) and $T_C = 190$ K (La_{0.5}Ba_{0.5}CoO₃). The obtained magnetic properties reveal mixed spin states of LS and IS of Co^{3.5+} (Co³⁺/Co⁴⁺) in both compounds. The ratio of LS state estimated from P_{eff} and saturated magnetization is higher in LaBaCo₂O₆ than in La_{0.5}Ba_{0.5}CoO₃. The lowering of T_C by 15 K in LaBaCo₂O₆ is due to a lower ratio of IS state with e_g -electrons responsible for ferromagnetic metal generated by DE interaction. Below about $T_i = 140$ K, both compounds exhibit structural change and magnetic glassy (cluster glass) behaviors. The refined structural data and electromagnetic properties suggest a

partial $d_{x^2-y^2}$ orbital ordering for LaBaCo₂O₆ below $T_1 = 140$ K, in contrast to a partial $d_{3z^2-r^2}$ orbital ordering for La_{0.5}Ba_{0.5}CoO₃. The $d_{x^2-y^2}$ orbital ordering in LaBaCo₂O₆ has a close relation to the structural characteristic that the CoO₂ layer is sandwiched by the two types of rock-salt layer, LaO and BaO, with different lattice sizes. The peculiar (noncentrosymmetric) distortion of CoO₆ octahedra is well relaxed by the $d_{x^2-y^2}$ orbital ordering.

Acknowledgements

The authors thank T. Yamauchi, M. Isobe, Y. Matsushita, K. Ohgushi and H. Ueda for valuable discussion. This work is partly supported by Grants-in-Aid for Scientific Research (No. 407 and No. 758) and for Creative Scientific Research (No. 13NP0201) from the Ministry of Education, Culture, Sports, Science and Technology.

- 1) S. Tsubouchi, T. Kyomen, M. Itoh, P. Ganguly, M. Oguni, Y. Shimojo, Y. Morii and Y. Ishii: *Phys. Rev. B* **66** (2002) 52418.
- 2) M. A. Senaris-Rodriguez and J. B. Goodenough: *J. Solid State Chem.* **116** (1995) 224.
- 3) M. A. Korotin, S. Y. Ezhov, I. V. Solovyev, V. I. Anisimov, D. I. Khomskii and G. A. Sawatzky: *Phys. Rev. B* **54** (1996) 5309.
- 4) H. Masuda, T. Fujita, T. Miyashita, M. Soda, Y. Yasui, Y. Kobayashi and M. Sato: *J. Phys. Soc. Jpn.* **72** (2003) 873.
- 5) P. Ravindran, P. Korzhavyi, H. Fjellvag and A. Kjekhus: *Phys. Rev. B* **60** (1999) 16423.
- 6) I. O. Troyanchuk, N. V. Kasper and D. D. Khalyavin: *Phys. Rev. B* **58** (1998) 2418.
- 7) T. Nakajima, H. Kageyama, H. Yoshizawa and Y. Ueda: *J. Phys. Soc. Jpn.* **71** (2002) 2843.
- 8) T. Nakajima, H. Yoshizawa and Y. Ueda: *J. Phys. Soc. Jpn.* **73** (2004) 2283.
- 9) D. Akahoshi and Y. Ueda: *J. Phys. Soc. Jpn.* **68** (1999) 736.
- 10) A. Maignan, C. Martin, D. Pelloquin, N. Nguyen and B. Raveau: *J. Solid State Chem.* **142** (1999) 247.
- 11) C. Frontera, J. L. Garcia-Munoz, A. Llobet, Ll. Manosa and M. A. G. Aranda: *J. Solid State Chem.* **171** (2003) 349.
- 12) M. Soda, Y. Yasui, M. Ito, S. Iikubo, M. Sato and K. Kakurai: *J. Phys. Soc. Jpn.* **73** (2004) 464.
- 13) F. Fauth, E. Suard and V. Caignaert: *Phys. Rev. B* **65** (2001) 60401.
- 14) F. Izumi and T. Ikeda: *Mater. Sci. Forum* **321-324** (2000) 198.
- 15) T. Nakajima, H. Kageyama, M. Ichihara, K. Ohoyama, H. Yoshizawa and Y. Ueda: *J. Solid State Chem.* **177** (2004) 987.
- 16) T. Nakajima, H. Kageyama, H. Yoshizawa, K. Ohoyama and Y. Ueda: *J. Phys. Soc. Jpn.* **72** (2003) 3237.
- 17) M. Itoh, I. Natori, S. Kubota and K. Motoya: *J. Phys. Soc. Jpn.* **63** (1994) 1486.
- 18) M. Itoh and I. Natori: *J. Phys. Soc. Jpn.* **64** (1995) 970.
- 19) Y. Motome and N. Furukawa: *J. Phys. Chem. Solids* **63** (2002) 1357.
- 20) R. Kajimoto, H. Yoshizawa, H. Kawano, H. Kuwahara, Y. Tokura, K. Ohoyama and M. Ohashi: *Phys. Rev. B* **60** (1999) 9506.